How do modern transportation projects impact on development of impervious surfaces via new urban area and urban intensification? Evidence from Hangzhou Bay Bridge, China

Abstract

Many countries have been constructing modern ground transportation projects. This raises questions about the impacts of such projects on urban development, yet there have been few attempts to systematically analyze these impacts. This paper attempts to narrow this information gap using the Hangzhou Bay Bridge project, China, as an exploratory case study. Using remotely sensed data, we developed a framework based on statistical techniques, wavelet multi-resolution analysis and Theil-Sen slope analysis to measure the changes in impervious urban surfaces. The derived changes were then linked to the bridge project with respect to socio-economic factors and land use development. The findings highlight that the analytical framework could reliably quantify the area, pattern and form of urban growth and intensification. Change detection analysis showed that urban area, GDP and the length of highways increased moderately in the pre-Hangzhou Bay Bridge period (1995-2002) while all of these variables increased more substantially during (2002-2009) and after (2009-2013) the bridge construction. The results indicate that the expansion of impervious surfaces due to urban growth came at the expense of permeable surfaces in the urban fringe and within rural regions, while urban intensification occurred mainly in the form of the redevelopment of older structures to modern high-rise buildings within existing urban regions. In the context of improved transportation infrastructure, our findings suggest that urban growth and intensification can be attributed to consecutive events which act like a chain reaction: construction of improved transportation projects, their impacts on land use development policies, effects of both systems on socio-economic variables, and finally all these changes influence urban growth and intensification. However, more research is needed to better understand this sequential process and to examine the broader applicability of the concept in other developing regions.

Key Words: Ground transportation infrastructure; impervious surfaces; Hangzhou Bay Bridge; wavelet multi-resolution analysis ; Theil-Sen slope; Consecutive events

1. Introduction

Throughout the history of civilization, ground transportation infrastructure has played a crucial role in the processes of urbanization and industrialization (Cai et al., 2013).This argument relies on the simple logic that one first needs to have access to markets and ideas before one can benefit from them (Banerjee et al., 2012). Countries that have powerful transportation infrastructure at national and regional scales attract not only local investment but global capital as well (Aksoy and Gultekin, 2006). For example, ground transportation infrastructure plays an important role in many regional development programs, such as those of the United States of America (Lein and Day, 2008), Europe (Thomas and O'Donoghue, 2013) and China (Zheng et al., 2016). In recent years, accelerating urbanization has led to further demand for updated and sustainable ground transportation infrastructure (Jha et al., 2014; Li, 2016). Such systems are characterized by shorter travel times, greater safety, energy efficiency and reduced environmental impacts (Kim and Han, 2016). Improved transportation systems play a major role in hastening urban, rural, industrial and economic development, and lead to the expansion of jobs, education and personal opportunities (Gunasekera et al., 2008; Tsou et al., 2015; Locatelli et al., 2017).

Although improved ground transportation infrastructure development usually takes into account environment protection issues (Li, 2016), these systems can lead to anthropogenic land use and land cover (LULC) change. In the main, the introduction of new or much improved transportation systems that lower commuting times and short-haul costs may attract new workers and/or industries which generally converts land from a less-intensive use to more intensive (Lein and Day, 2008). There has been a wealth of literature documenting the impacts of ground transportation on LULC change using the combination of remotely sensed data, Geographic Information Systems and landscape metrics (Badoe and Miller, 2000; Serrano et al., 2002; Lein and Day, 2008; Aljoufie et al., 2013a; Aljoufie et al., 2013b; Bruschi et al., 2015; Tsou et al., 2015). However, these studies have focused mainly on the decline of agricultural land and loss of biodiversity caused by ground transportation projects. While this is important in many regions, few studies have sought to evaluate how improved ground transportation infrastructure influences the extent and spatial distribution of impervious surfaces.

Understanding the impacts of improved transportation projects on impervious surfaces is of great importance in growth management and sustainable planning because impervious surfaces- including roads, railways, built-up areas and parking lots- comprise most human dominated landscapes and their expansion can pose a range of insurmountable environmental challenges, primarily due to changing surface energy balances, hydrological systems and biogeochemical cycles(Weng, 2008; Weng, 2012). The growth of impervious surfaces is generally divided into two forms: inter-class and intra-class changes (Yang et al., 2003; Yang and Liu, 2005; Rashed, 2008; Michishita et al., 2012; Shahtahmassebi et al., 2014; Shahtahmassebi et al., 2016). As shown in Fig.1, inter-class change is related to the transformation of non-built lands into impervious surfaces and it reflects urban growth (Yang and Liu, 2005; Michishita et al., 2012). If new impervious surfaces occur around the edge of existing urban regions and along highways, this signifies urban expansion while if new impervious surfaces occur within urbanized areas, this indicates the process of infilling (Shahtahmassebi et al., 2014). In general, expansion and infilling mechanisms cause a carpeting phenomenon (formation of continuous

impervious surfaces) (Shahtahmassebi et al., 2014). Intra-class change indicates a change in the proportion of impervious surface cover (Yang et al., 2003; Yang and Liu, 2005). It is notable that urban growth and urban intensification can increase the proportion of impervious surface cover. However, urban intensification can also lead to a decline in impervious surface cover over time as dense low-rise urban structures are replaced by modern high-rise buildings interspersed with new green open spaces, as evidenced in Figure 1. This form of redevelopment has been observed by a number of studies within city centers and existing urbanized regions (Rashed, 2008; Michishita et al., 2012; Shahtahmassebi et al., 2014; Shahtahmassebi et al., 2016).

Both urban growth and urban intensification present daunting problems for planners and policy-makers. In urban growth, land lost to new impervious surfaces may compromise green spaces within cities, agricultural land and water conservation areas in the urban fringes (Weng, 2012). Urban intensification causes modification of the neighborhood morphology within urbanized areas, thereby having possible impacts on surface and ground water, urban ecology, urban demographics and urban structure (Shahtahmassebi et al., 2016). To address these issues, there is currently increasing interest and debate in understanding the forces that influence changes in impervious surfaces (Weng, 2012; Ma et al., 2016; Song et al., 2016c). A number of case studies have identified two major drivers: land use regulations (Stone, 2004; Sung et al., 2013) and socioeconomic factors (Michishita et al., 2012; Ma et al., 2016). Although these studies focused on either single factors (e.g. highways) or multiple factors (e.g. highways and Gross Domestic Product(GDP)) at different scales (e.g. provinces and counties), there are few analyses which look at the growth of impervious surfaces as a result of consecutive events or chain reactions. For example, it is interesting to understand systematically the degree to which improved or advanced transportation systems have contributed to changes in impervious surfaces (through urban growth and intensification) (Fig. 1). Given that many countries have concentrated on constructing improved ground transportation systems such as high speed rail, super highways and mega sea bridges, there is an urgent need to systematically examine the impacts of such projects on urban growth and urban intensification.
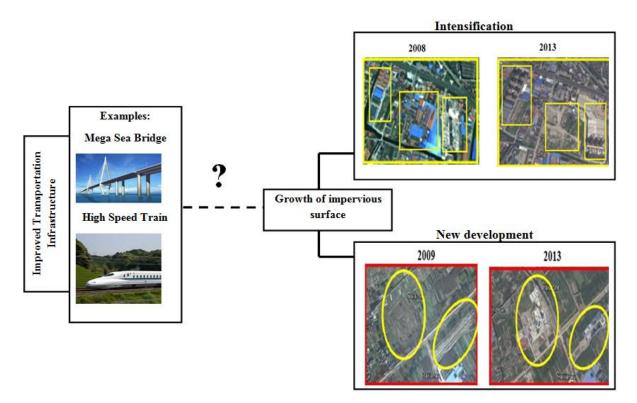
Fig.1 What is the interaction between improved transportation projects and urban growth and urban intensification?

In this respect, China is an example of a present-day state that has experienced significant modernization of ground transportation infrastructure (Zheng et al., 2016). Before economic reform in 1978, the transportation system was inefficient even though it was partially modernized, but since the early 1990s, China has invested in the development of efficient and updated ground transportation infrastructure in response to its rapid growth in population and economy (Loo, 1999; Wilkins and Zurawski, 2014). These systems aim to integrate economic development, resource use efficiency and environmental protection; these integrated Chinese policy aims have been coined as the dual goal society (Jia et al., 2012; Song et al., 2016b). Components of the modern Chinese transportation system include expressways, high speed railways and sea bridges. A review of these components has been given by Zheng et al. (2016). Several regional studies have focused on the relationship between urban growth, regulatory activities (Michishita et al., 2012; Sung et al., 2013; Shahtahmassebi et al., 2014; Shahtahmassebi et al., 2016) and land use policies (Lichtenberg and Ding, 2008). However, less attention has been devoted to understanding how the construction of updated ground transportation infrastructure leads to the implementation of urban growth policies and consequently the increase in impervious surfaces.

This paper aims to improve our understanding of how transportation construction projects influence urban growth and urban intensification. To do so, this study contributes in two crucial aspects in the context of transportation projects and land use policy. First, we propose a cascade framework using statistical analysis, multi-resolution analysis (MRA) and digital change detection to capture urban growth and urban intensification.

Secondly, we systematically link derived changes to an improved transportation project by integrating major transportation regulations, socio-economic variables and land use policy developments. To examine this relationship, Hangzhou Bay Bridge was selected as a typical example of a major advanced transportation development in China. We scrutinized impervious surface change in a representative buffer zone in periods before (1995-2002), during (2002-2009) and after (2009-2013) construction of this mega sea bridge. Through a detailed assessment of impervious surface change in the region, the potential for future urban growth was better defined and avenues for further investigation were identified. Additionally, this baseline investigation provided a methodology to guide more detailed assessments of the policy instruments used to promote ground transportation investment as a means of encouraging regional economic development.

1.1 Research questions:

This study attempts to address the following questions:

1) What are the benefits of continuous change detection methods (i.e. our proposed method) for quantifying urban growth and intensification?
2) How do transportation construction projects impact urban growth and intensification?
3) Is urban growth and intensification the direct result of such projects or an indirect effect?

1.2 Research framework: continuous change detection

In the context of land use policy research several studies have used thematic mapping techniques to examine the impacts of transportation infrastructure projects on urbanization or the development of impervious surfaces (Su et al., 2014; Song et al., 2016a; Zheng et al., 2016). However, thematic map techniques are unable to measure the full continuum of impervious surface changes induces by urban growth and urban intensification. If changes in impervious surfaces can be quantified using continuous surface maps (as opposed to thematic maps) to characterize spatial distribution, pattern and temporal variation, this can yield comprehensive information to help understand the causes of change (Powell et al., 2007; Rashed, 2008; Song et al., 2016c). However, there is little evidence of the treatment of impervious surface change as a continuous process in land use policy research (Stone, 2004; Sung et al., 2013; Ma et al., 2016). Moreover, little attention has been paid to understanding the potential impacts of improved ground transportation on impervious surface change using continuous mapping techniques.

Therefore, it is imperative to develop a framework which takes into account technique development and policy assessment. In terms of technique, we need to develop a continuous framework which simultaneously decomposes change in impervious surfaces into urban growth and urban intensification. In particular, the framework should quantify the pattern, type and spatial distribution of decomposed changes in informative and comprehensive ways. With respect to the impact assessment, decomposed changes should be systematically scrutinized before, during and after construction of improved ground transportation along with land use development policies and socio-economic variables at the study site. We contend that in the context of land use policy research this framework could provide a more comprehensive picture of impervious surface change than

that offered by the more limited thematic techniques.

To achieve this, we propose a framework which includes two stages: quantifying change and analyzing observed change (Fig 2). In quantifying change (Stage 1), we develop a three-step approach that combines statistical analysis, wavelet multi-resolution analysis (MRA) and digital change detection to quantify the growth of impervious surfaces over time. Here, the first step calculates the area of new development and categories of impervious surface fractions. The second step quantifies new development and intensification of impervious surfaces over time while the third step determines the spatial pattern and type of impervious surface growth. In analyzing observed change (Stage 2), we analyze the growth of impervious surfaces with respect to the improved ground transportation by integrating land use development policy and socio-economic variables.
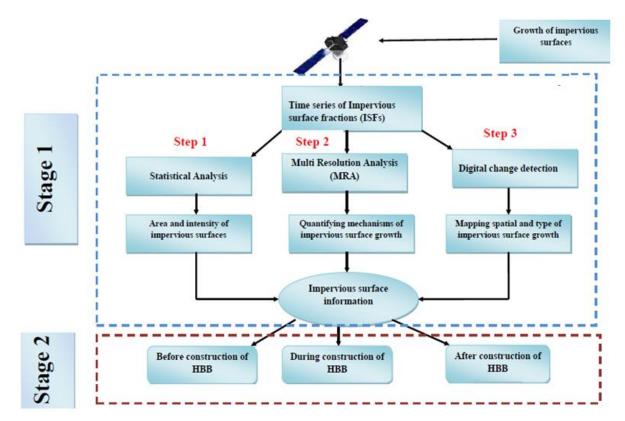

Fig.2. Analytical workflow. Stage 1: quantifying change of impervious surfaces. Stage 2: analyzing observed change. HBB is an abbreviation of Hangzhou Bay Bridge.

2. Case Study: Hangzhou Bay Bridge and Cixi County

To answer the research questions, we selected the Hangzhou Bay Bridge as a representative of modern Chinese transportation systems and focused on Cixi County to monitor change in impervious surfaces before (1995-2002), during (2002-2009) and after the construction of the bridge (2009-2013). Hangzhou Bay Bridge is the third longest ocean-crossing bridge in the world with an overall length of 36km (Zheng et al., 2016). The preparatory work was conducted between 1994 and 2003, construction began in June 2003 and the bridge was completed in June 2007. The accessibility of Cixi County to other regions of China had previously been handicapped by mountains to the south and Hangzhou Bay to the north (Fig.2). Given that a part of Hangzhou Bay Bridge is located in Cixi County, opening the bridge may have encouraged growth of impervious surfaces. Previous studies have analyzed the spatial distribution and pattern of impervious surface growth in Cixi County (Shahtahmassebi et al., 2012; Shahtahmassebi et al., 2014). However, those studies did not quantify the impacts of the Hangzhou Bay Bridge construction on the change in impervious surfaces. Zheng et al. (2016) mapped the change in the area of impervious surface in Cixi County using conventional techniques before (1995-2002) and during (2002-2009) construction of Hangzhou Bay bridge but not after construction, and they did not account for both urban growth and intensification processes.

In order to comprehensively assess the possible impacts of the Hangzhou Bay Bridge on urban growth and intensification in Cixi County, and to minimize the influence of other factors such as neighboring counties on these changes, we limited the focus of this study to a buffer zone with a length of 42km and a width of 4 km along the Cixi Development Zone which is connected to the Hangzhou Bay Bridge (Fig. 3). This buffer zone was derived from the Cixi County master plan map (Cixi_Government, 2003). Since the aim of this research was to examine the impacts of advanced transportation developments on urban growth and intensification, we do not present details of this master plan here, nor do we evaluate its performance.
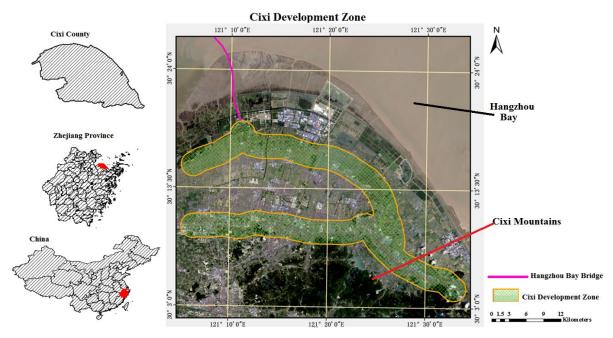

Fig.3. Study area, Cixi Development Zone(CDZ). The background satellite image is from Landsat OLI, acquired on 12[th]July2013 in false color composite (Bands 4,3,2).

3. Method

3.1 Pre-processing

Four Landsat images covering the study site were acquired, which had been geometrically corrected and registered. These images were divided into two groups: previously derived Impervious Surface Fraction (ISF) images and an original Landsat image. The ISF images were derived from a previous project (Shahtahmassebi et al., 2014) using a Landsat5 TM image from 13 September 1995, a Landsat7 ETM + image from 11 November 2002 and a Landsat5 TM image dated 10 October 2009. The ISFs images were computed by applying Multiple Endmember Spectral Mixture Analysis (MESMA) to these data sets (see Shahtahmassebi et al., 2014 for full methods and accuracy assessment). In terms of the original image, a Landsat8 OLI scene image acquired on 12 July 2013 was used for impervious surface estimation. We used similar image preprocessing to that applied to the Landsat 1995, 2002 and 2009 images(Shahtahmassebi et al., 2014), using ENVI RSI 5.1. The panchromatic, thermal and coastal bands of Landsat8 OLI were excluded from the analysis.

The boundary polygon of the Cixi Development Zone, which was provided by a local government website (Cixi Government Website, 2003), was separately applied to individual images in order to derive data for this region at a given point of time. Additionally, cities and rural boundaries in 2010, Google Earth images (2008-2014) and socio-economic data (1995, 2002, 2009 and 2013) were also collected for analytical purposes. Socioeconomic statistics were derived from Zhejiang Statistical Year Books for 1996, 2003, 2010 and 2014. These data consisted of registered population, non-agricultural population, GDP, GDP in secondary industry, GDP in tertiary industry and total length of highways. The selection of these socioeconomic statistics was based on their relationships with impervious surface growth, as demonstrated in previous studies (Michishita et al., 2012; Ma et al., 2016).

3.2 Estimating Impervious surfaces using the Landsat 8 OLI image

MESMA has been used successfully for mapping impervious surfaces from remotely-sensed imagery due to its potential to characterize the complex spectral variability in urban land covers (Lu and Weng, 2006; Rashed, 2008; Powell and Roberts, 2008a; Demarchi et al., 2012). The basic concept of MESMA is that the reflectance measured within a pixel is the linear sum of N pure spectra named endmembers (Powell et al., 2007). The number and type of endmembers are allowed to vary on a pixel-by-pixel basis, addressing the issue of spectral and spatial variability (Roberts, 2007). The efficiency of MESMA has been demonstrated in Cixi County in previous studies (Shahtahmassebi et al., 2012; Shahtahmassebi et al., 2014). In this context, the MESMA steps for estimating ISF from the Landsat8 OLI image were similar to those former studies in Cixi County. The MESMA steps were: (1) Candidate endmember extraction; (2) Developing a spectral library; and (3) Spectral un-mixing by MESMA. These steps were implemented with VIPER Tools, a plug-in for ITT ENVI (Roberts, 2007; Michishita et al., 2012; Shahtahmassebi et al., 2012; Shahtahmassebi et al., 2014; Shahtahmassebi et al., 2016).

Candidate endmember extraction

Endmember land cover features were derived from the Landsat8 OLI image using supervised visual interpretation and through use of a minimum noise fraction (MNF) transform (Lu and Weng, 2006). The image endmembers were divided into four major groups: vegetation cover, photometric shade, impervious surfaces, and bare soil (Table 1). The shade endmember was used to account for variation in illumination (Dennison and Roberts, 2003). The collected endmembers were transferred into VIPER Tools in order to construct a spectral library.

Table1 Number of endmembers for each class. Selected endmembers were chosen following the optimization process outlined in Step 2.

Class	Impervious surface	Soil	Vegetation cover
Total	27	27	27
Selected	5	8	3

Developing a spectral library

As suggested in previous studies, optimal endmember spectra were selected from the spectral library using three optimization indices: CoB (Count Based selection), EAR (Endmember Average Root Mean Square Error) and MASA (Minimum Average Spectral Angle)(Roberts, 2007). Optimal spectra are defined as those spectra within a library that are most representative of their class while covering the range of variability within that class (Table 1).The optimum spectrum had the highest CoB, lowest EAR and lowest MASA (Roberts, 2007). In Cixi County, the following modeling conditions were applied to the calculation of these indices: maximum RMSE (0.025), maximum fraction (1.05) and minimum fraction (-0.05)(Shahtahmassebi et al., 2014).

Spectral un-mixing by MESMA

MESMA was used to un-mix each pixel in the image by evaluating all possible combinations of spectra included in the spectral library (Table 1). The combination of total and selected endmembers used in the MESMA modeling is presented in Table 2. The minimum and maximum endmember fractions were -0.05 and 1.05, respectively (Michishita et al., 2012). By allowing endmember fractions slightly greater than 1.00 and slightly less than 0.00, MESMA was able to take into account models that fit well in spite of endmember fractions that were somewhat physically unrealistic (Thorp et al., 2013). Then the values between 0 and 1 were selected from the ISF image for 2013 and the earlier ISF images (i.e.1995,2002 and 2009). It is noteworthy that soil and vegetation fractions were used only in this section to accurately identify impervious surfaces; in the remainder of the study these endmembers and corresponding fractions were excluded from the investigation of urban growth and intensification, as we concentrated only on impervious surface change. Further ISF images

were labeled to the range between 0 and 100. This range was only used for visual inspection (as a legend) while the original range was employed for the numerical analysis.

Table2 Detail of MESMA model parameterization

Year	Total EM[1]	Number of selected EM[2]	Type of combination[3]	Number of models[4]
2013	81	15	4-Endmembers	120

[1]*Total endmembers calculated; see Table 1.*

[2] *Selected optimal endmember spectra.*

[3]*Number of spectral libraries added to the model.*

[4]*The number of models was calculated as the number of impervious surface spectra × the number of vegetation spectra × the number of soil spectra.*

3.2.1   Accuracy assessment

We utilized color aerial photography with a spatial resolution of 2m acquired in 2013 as reference data to assess the accuracy of the ISF image derived from the 2013 Landsat8 OLI image. The geographic extent of the 2013 aerial photography covered a portion of the Cixi Development Zone with a range of land cover types, including farm land, industrial, rural residential and urban residential.

The sequential Support Vector Machine (SVM) of ENVI RSI 5.1 was implemented to classify the reference imagery into two classes: impervious surface and pervious covers. The technical setting parameters of this approach were: Radial Basis Function for Kernel Type, Gamma in Kernel Function (0.33), Penalty Parameter (100.00), and Pyramid levels (0). The total number of training samples was 600 and 700 for impervious surface and pervious surface features, respectively. The SVM was carried out in two sequences. First, agricultural lands were removed from the imagery, then soil and water classes were extracted. The final overall accuracy of the classification was found to be 97% based on a cross-comparison with visual inspection of samples, and this illustrated that this high spatial resolution binary image was a suitable reference for assessing the Landsat8 OLI-derived ISF image.

A 3×3 pixel (90m×90m) sampling plot was selected to reduce the impacts of geometric errors associated with both the OLI image and the aerial photography (Wu, 2004). Then 313 randomly located plots from the binary reference image were extracted with the Grid Analysis technique in ERDAS Imagine 2011. For detailed analysis, the sample plots were subdivided into two categories: plots over the urban centre (224 samples) and plots in the suburbs (89 samples). Within each plot, all 2m pixels classified as impervious surfaces in the binary reference were enumerated to determine the percentage of imperviousness.

ISF values estimated by MESMA from the Landsat8 OLI image were plotted against reference ISF values derived from the high-resolution aerial photography. Measures of accuracy included the slope, intercept,

coefficient of determination (R^2) of the regression relationship, and Pearson's (r) correlation coefficient. Additionally, Root Mean Square Error (RMSE) and bias were employed to examine the range of disagreement between fraction estimates and reference data, where RMSE measures the overall estimation accuracy for all samples and bias is the average of the error, indicating general trends in over-and under-estimation (Powell and Roberts, 2010).

3.3 Data analysis

3.3.1 Statistical analysis- Newly developed impervious surface and categories of impervious surface fractions

Urban land cover in the Cixi Development Zone was characterized by the presence of impervious surface cover. To provide statistical information on change in impervious surfaces, we used two measures: (a) area of newly developed impervious surface and (b) area of different categories of ISF. In terms of first measure, we counted the number of pixels with an ISF greater than zero (a measure of the "pixelized" area with impervious surface present, regardless of the fraction magnitude) at an earlier time(t1) and a more recent time(t2)(Powell and Roberts, 2010). Then the number of pixels was converted into an area by multiplying by the area of a Landsat pixel ($900m^2$). Finally, the difference between t1 and t2 was calculated to represent the change in impervious surface area.

With respect to the second metric, a Decision Tree Classifier (DTC) was separately applied to individual ISF images in order to map 10 categories of ISF at a given point in time. Each ISF image was classified by 10 decision rules into ISF categories: 0-10%, 11%-20%, 21%-30%, 31%-40%, 41%-50%, 51%-60%, 61%-70%, 71%-80%,81%-90%, and 91%-100%. DTC rules were built in ENVI RSI version 5.1. Then the area of each category was computed and the mean ISF for those pixels with non-zero ISF was calculated for individual ISF images so as to present an overall measure of the magnitude of ISF (Powell and Roberts, 2010).

3.3.2 Quantifying urban growth and urban intensification by multi-resolution analysis

Time series of ISFs are usually non-stationary, i.e. they present different frequency components such as abrupt changes, subtle changes, long term trends and short term fluctuations. In addition, such series can be contaminated by sensor and atmospheric noise. In this context, Wavelet Transform (WT) based methodologies may be beneficial because of their ability to process signals with different frequency components and their power in smoothing time series. For time series analysis, multi-resolution analysis (MRA) based on WT is commonly used because it offers the possibility of capturing the presence of the short-lived (high frequency) variability, such as abrupt changes, while also resolving processes that show low frequency variability over time.

The fundamental idea behind wavelets is to analyze a signal according to different time scales or resolutions. A WT uses local basis functions (wavelets) that can be stretched and translated with a flexible resolution in both frequency and time domains (Percival and Walden, 2000). A WT may be continuous or discrete. In the case of MRA, a discrete wavelet transform (DWT) is used in a hierarchical algorithm, otherwise known as a pyramid

algorithm (Mallat, 1989). The DWT, specifically implemented for discrete signals, allows for a decomposition of the signal into time scales based on powers of two, $a=2^j$ ($j=1,…m$), also known as dyadic sampling, where m is the highest decomposition level considered. As a result of the MRA, the original signal $f(t)$ can be reconstructed as(Martinez et al., 2011):

$$f(t) = A_m(t) + \sum_j^m = 1D_j(t) \tag{7}$$

Where A is the approximation component and D the detail component. In the first level of the decomposition, $f(t)=A_1+D_1$, the signal has a low-pass filtered component, A_1, and a high-pass filtered component, D_1. In the second level, the approximation A_1 is split as $A_1=A_2+D_2$, and so on. The detail component, $D_j=A_j-1-A_j$, gives us information about the portion of the signal that can be attributed to variations between the time scales associated with the levels [$j-1, j$], whereas the A_m component is associated with averages over time scales 2^m and longer and, therefore captures the slowly varying portion of the original signal (Percival and Walden, 2000).

Several wavelet functions can be found in the literature with different characteristics. In this study, the Meyer orthogonal discrete wavelet was chosen because previous studies have demonstrated successful results with this wavelet in land-cover change analysis using MRA of time series of Moderate Resolution Imaging Spectro radiometer (MODIS) images (Freitas R.M and Y.E., 2008) and Advanced Very High Resolution Radiometer (AVHRR) imagery (Martinez and Gilabert, 2009). These studies showed that time series of NDVI can be divided into two parts by MRA: new regions or inter-change (i.e. approximation component) and intensification or intra-change (i.e. detail component)(Lindsay et al., 1996; Hubbard, 1998; Percival and Walden, 2000; Galford et al., 2008; Martinez and Gilabert, 2009). Based on these findings, it follows that similar results may be obtained for the analysis of time series of ISF using MRA.

In order to select the most appropriate level for the MRA components, the maximum wavelet decomposition level was used. This function returns the maximum level decomposition of a signal of size S using the named wavelet (herein "Meyer"). In this study, MRA was applied to the ISF series to decompose the original series into areas of urban growth (approximation component) and urban intensification (detail component). More detailed evaluations of MRA can be found elsewhere (e.g. Percival and Walden, 2000; Lindsay et al., 1996; Burke-Hubbard, 1998).

3.3.3 Digital change detection

The third step of the data analysis was mapping the spatio-temporal characteristics of impervious surface change. Given that ISF images might be contaminated by noise due to environmental effects, different sensors, and artefacts of the MESMA procedure, we adopted an image regression technique to minimize such effects (IDRISI, 2012; Castrence et al., 2014). Many image regression techniques have been suggested, among which the Theil-Sen (TS) slope method has been shown to be robust with respect to noise and outliers; it can tolerate arbitrary corruption of up to 29.3% of the input data without degradation of its accuracy (Chu et al., 2015). The TS slope is calculated by determining the slope between every pair wise combination and then finding the median values. In this study, two ISF images from consecutive study years were utilized to calculate each TS slope image. The formula is as follows:

$$S_{ISF} = \text{median} \left(\frac{ISF_j - ISF_i}{j - i} \right), \tag{8}$$

Where S_{ISF} refers to the TS median of ISF, and ISF_i and ISF_j represent the ISF values of years of i and j. In general a TS slope > 0 means a gain in ISF while a TS slope < 0 indicates a loss. Changes in ISF values can be generated by two processes: urban growth and urban intensification. Urban growth involves the conversion of non-urban covers (i.e. zero pixels) into impervious land, which can be identified by positive S_{ISF} slope values. Urban intensification is characterized as change within existing urban areas due to the replacement of old features with new ones, which typically involves demolishing low-rise built-up areas and replacing these with mixtures of high-rise buildings and other types of land cover such as vegetation. Hence, urban intensification results in low magnitude S_{ISF} slope values which could be positive or negative. Since the aim of this research was to analyze the fine scale effects of transportation infrastructure on urban dynamics, we did not evaluate the TS slope methods, for example by employing a trend test such as Mann Kendall (Jiang et al., 2015). However, the results from this method were assessed by comparison with a visual interpretation of a time series of high resolution imagery from Google Earth.

4.Results

4.1 Accuracy Assessment

Descriptive statistics for the reference and estimated ISFs are furnished in Table 3. The results indicate that the MESMA technique was effective for estimating ISF. There is a strong correlation between the reference and estimated ISFs in both the urban centre and suburbs, with slopes of approximately 0.90, r of 0.95 and R^2 of 0.90 (Table 4). There are good overall RMSE values of 8.6% and 7.7% for samples in the suburbs and urban centre, respectively. Furthermore, the analysis of bias illustrates that no significant estimation bias exists for all sample areas. The graphic analysis showed that MESMA both under-estimated and over-estimated slightly in the 0.2-0.4 ISF region (Fig. 4a&c). The standardized residuals indicated that about 95% of data is located between -2 and +2 (Fig. 4-b, d) and that possible outliers are situated between 0.2-0.4. Based on these results the accuracy of the 2013 ISF data was comparable with that of the ISF data for previous years (Shahtahmassebi et al., 2014) and was therefore considered suitable for use in the subsequent analyses.

Table 3 Summary measures for actual and modeled fractions

	Suburbs		Urban Centre	
	Reference IS*	Modeled IS	Reference IS	Modeled IS
Minimum	0.01	0.08	0.01	0.01
Maximum	0.99	0.99	1.00	1.04
Mean	0.54	0.58	0.75	0.78
Standard Deviation	0.30	0.28	0.22	0.21

IS: Impervious surface

Table 4 Accuracy assessment

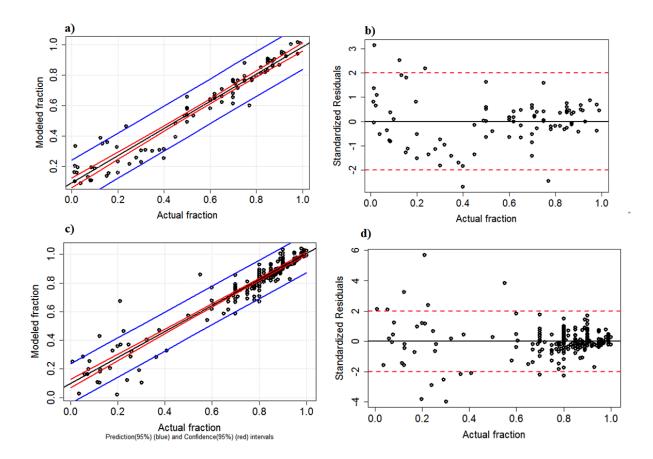| Metrics	Suburbs	Urban Centre
Slope	0.89	0.90
Intercept	0.09	0.09
R^2	0.93	0.91
Pearson's r	0.96	0.95
RMSE	8.6%	7.7%
Bias(SE)	3.4%	2.8%

Fig.4. Comparison between reference and modeled impervious surface fractions: (a) correlation plot for the suburbs, (b) standardized residuals for the suburbs, (c) correlation plot for the urban centre and (d) standardized residuals for the urban centre.

4.2 Visual inspection of ISF images

Four ISF images (i.e. 1995,2002,2009 and 2013), with values ranging from 0 to 100, were derived from

14

corresponding Landsat data using MESMA (Fig 5). Visual inspection of the four images for the different dates helped to reveal new urban development, and the direction and magnitude of change in built-up land cover. For example, a portion of the Cixi Development Zone highlighted by a square in the ISF images indicates an area that has experienced considerable urban growth. In contrast, in the area highlighted by the circle the built-up extent remained approximately constant between 2009 and 2013, but there was a distinct increase in the ISF, probably corresponding to increased building density. Overall, visual comparison shows a sharp increase in the fractional cover and extent of impervious surface after 2002 (Fig.5). In addition, the frequency histogram confirms proliferation of impervious surface pixels, especially in ISF categories greater than 50% in 2009 and 2013 (Fig.6). More importantly, the 2013 ISF image had considerably more impervious surface pixels than the 1995, 2002 and 2009 ISF images, with a notable abundance of low-medium ISF pixels (10%-40%)(Fig.6).
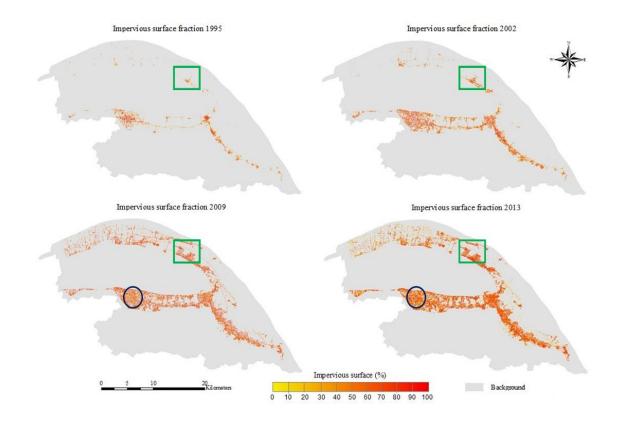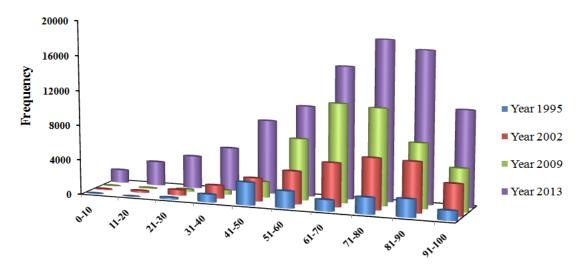

Fig.5. ISF images in the Cixi County buffer area in 1995, 2002, 2009 and 2013.

Fig.6. Frequency histograms of impervious surface pixels in the Cixi County buffer in 1995, 2002, 2009 and 2013.

4.3 Statistical analysis- Newly developed impervious surface and categories of impervious surface fractions

Impervious surfaces in the Cixi Development Zone increased substantially during the study period (Table 5-a). Between 1995 and 2002 the extent of impervious surfaces increased from 1090.4 ha to 2616.3 ha. Within cities and rural areas, impervious surfaces were expanded by 1195.02 ha and 140.58ha, respectively (Table 5-b). In terms of categories of impervious surface fractions, most impervious surface growth in cities was characterized by rapid modification in the 60-100% ISF classes (Fig.7-a). The categories of impervious surface fractions in rural areas remained relatively stable during this time period (Fig.7-b). This finding suggests that rural impervious surfaces had lower density than that of cities and also less land was consumed in rural areas for expanding impervious surfaces.

In the second time period (2002-2009), the extent of impervious surface increased from 2616.3 ha to 3989.52 ha. Impervious surfaces expanded by 477.9 ha and 432 ha in cities and rural areas, respectively (Table 5-b). Most urban regions were dominated by the 50-70% impervious surface categories (Fig.7 a). For rural areas, the greatest categories occurred in the 50-100% classes. For example, the area of 60%-70% impervious surfaces rose by 150 ha in these regions between 2002 and 2009(Fig.7-b). The greatest difference between impervious surface growth from first period (1995-2002) and second period (2002-2009) was the shift of new development and impervious surface categories from cities to rural areas.

During the third period, a remarkable expansion in impervious surface was observed, from 3989.52ha in 2009 to 8426.97 ha in 2013. Impervious surfaces increased by 2402.28 ha and 592.28 ha in cities and rural areas, respectively (Table 5-b). The 70-100% impervious surface fraction categories were most prevalent in both cities

16

and rural regions (Fig.7-a and b). Moreover, both cities and rural regions witnessed the growth of low-medium density developments.

Table 5 Extent and new development of impervious surfaces
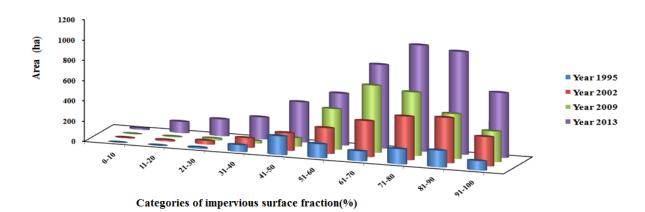
a) For the buffer

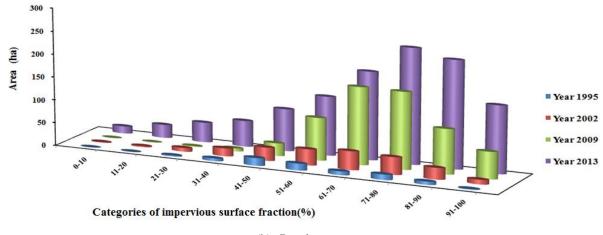| Year	Extent of impervious surface[1] (ha)	Change in impervious surface (ha) (t2-t1)[2]
1995	1090.4	—
2002	2616.3	1525.9
2009	3989.52	1373.22
2013	8426.97	4437.45

b) Within cities and rural areas

Year	Extent of impervious surface[1] in cities (ha)	Change in impervious surface in cities (t2-t1)[2]	Extent of impervious surface[1] in rural areas (ha)	Change in impervious surface in rural areas (ha) (t2-t1)[2]
1995	919.71	—	71.01	—
2002	2114.73	1195.02	211.59	140.58
2009	2592.63	477.9	643.59	432

| 2013 | 4994.91 | 2402.28 | 1236.51 | 592.92 |

[1]*Extent of impervious surfaces was calculated based on the number of pixels with an ISF greater than zero.*
[2] *t1: an earlier time and, t2: a more recent time*
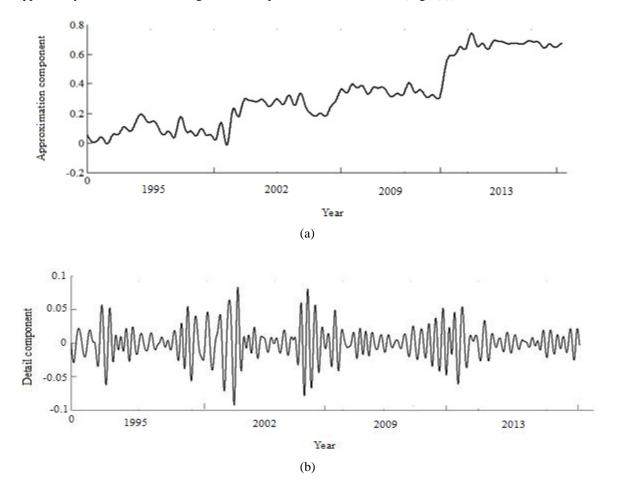

(a) Cities

(b) Rural areas

Fig.7. Changes in impervious surface area for different categories of ISF in (a) cities and (b) rural areas of the Cixi Development Zone in 1995, 2002, 2009 and 2013.

4.4 Quantifying urban growth and urban intensification using MRA

Fig.8(a) and (b) show the results of the MRA of the ISF time series in Cixi County buffer zone over time. The figure shows that the MRA decomposes the original signal into inter-class (Fig.8(a)) and intra-class changes (Fig.8(b)). The inter-class change corresponds with urban growth, i.e. between-class modification such as conversion of farm land to impervious surfaces. Inter-class changes indicated that there was a slight increase in urban area between 1995 and 2009. However, urban growth was marked between 2009 and 2013.

Intra-class change is associated with urban intensification, i.e. changes in impervious surface fraction in existing urban areas. The observed intra-class changes indicated that first period (1995-2002) experienced sharp intensification while a steady increase in intensification took place in the second period. Interestingly, the intensity of impervious surface decreased gradually in the last period (2009-2013). This result was also supported by the results for the magnitude of impervious surface fraction (Fig.8(c))
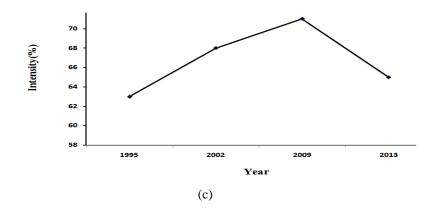

(a)

(b)

(c)

Fig.8. Temporal changes in (a) Urban growth (inter-class changes), (b) Urban intensification (intra-class changes), and (c) Magnitude of impervious surface fraction

4.5 Spatial patterns of urban growth and intensification

Fig.9 presents the dynamics of impervious surface growth based on an analysis of the TS slope (S_{ISF}). Comparison between these images, ISFs (Fig. 5) and time series images from Google Earth highlighted distinctive patterns and areas of urban development, both through intensification of existing urban lands and through the construction of new urban areas. Such comparisons confirm that areas of urban growth are highlighted by positive values in the S_{ISF} image, while areas of urban intensification generated negative or moderately positive S_{ISF} values. For example, Fig 9 shows an area of urban growth towards the edge of the existing urban regions dominated by the conversion of pervious lands to impervious surfaces. This is where former agricultural lands have been used for impervious surface development, which generates predominately large positive values of S_{ISF}. Intensification can observed in the urban core, where a continual cover of buildings and roads has been replaced by high-rise construction interspersed with some open spaces generating largely moderate positive and negative values in the S_{ISF} image. Moreover, no-change regions were notable for very low magnitude S_{ISF} values. Based on this comparison, we observed four major patterns before (1995-2002), during (2002-2009), and after (2009-2013) Hangzhou Bay Bridge construction: changing fraction of impervious surfaces in urban areas, urban edge growth, urban infilling and impervious surface carpeting (conurbation), and these are examined in detail below.
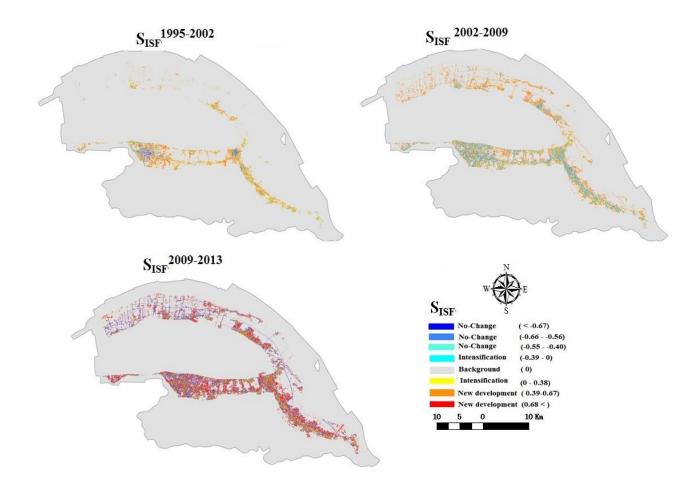
Fig.9. Theil–Sen slope values for impervious surface changes in the Cixi Development buffer zone from 1995 to 2013.

The first pattern of growth was characterized by the changing fraction of impervious surfaces within existing urban areas (Fig.10, small rectangles in black and yellow inside the big rectangles). Low magnitude S_{ISF} values highlighted this types of modification, suggesting that impervious surfaces changed modestly or decreased in urban regions during the study period. This phenomenon of urban intensification reflects a redevelopment process involving the transition from old and dense urban structures to contemporary urban living environments that are comprised of high-rise buildings and interspersed green spaces, as show in Figure 10. This pattern was mainly observed between 2009 and 2013.
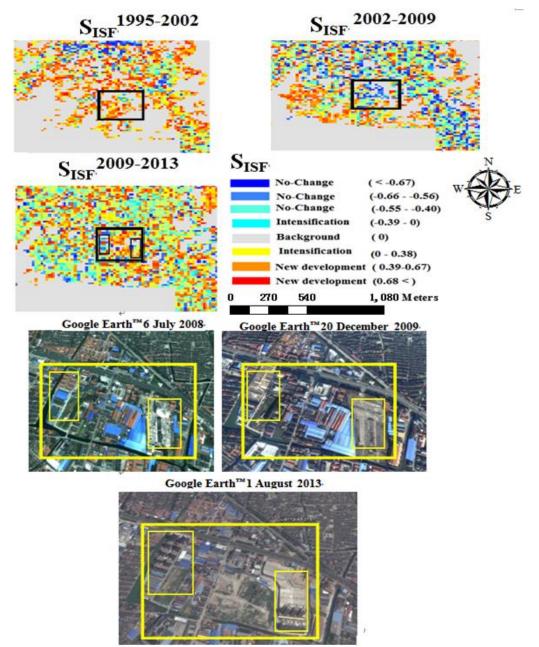
Fig.10. A portion of the Cixi Development Zone illustrating changing fraction of impervious surface cover within existing urban regions through urban intensification (old and dense urban structures have been replaced by high-rise urban living environments), the coordinate of this location is (30°09 ′51.96″N, 121°24′19.94″E)

The second pattern of impervious surface growth was edge growth (Fig. 11). This pattern was notable for positive S_{ISF} values. This pattern was most prevalent in urban peripheries and was the most common source of urban growth in the Cixi Development Zone. Edge growth occurred before, during and after construction of the Hangzhou Bay Bridge, and was particularly obvious during 1995-2009 and 2009-2013.
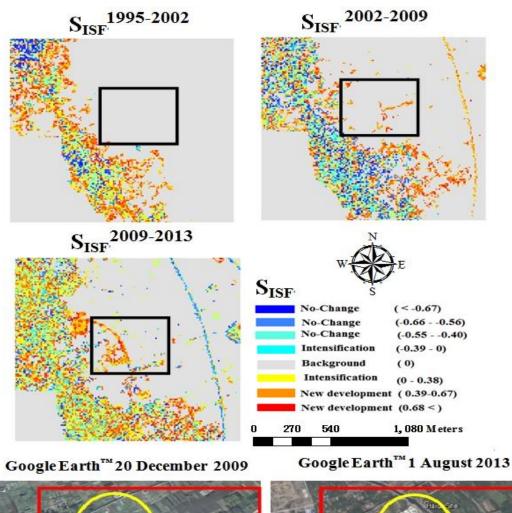
Fig.11.A portion of Cixi Development Zone illustrating new urban developments at the margin of existing urban areas, the coordinate of this location is (30°09′56.30″N, 121°25′22.33″E)

The third form of impervious surface growth was infilling of formerly open spaces within existing urban areas. As shown in Fig.12, the open spaces were initially fragmented between 1995-2009, then the fragmented gaps between the existing roads and urban regions were filled by impervious surfaces in the period 2009-2013.

The fourth pattern of growth was conurbation, termed impervious surface carpeting. This is because edge growth and infilling have led to the merger of impervious surface patches and contributed to the formation of large and continuous impervious surface cover. This pattern was notable for the latter period (2009-2013), as evidenced in Fig.12-entire image.
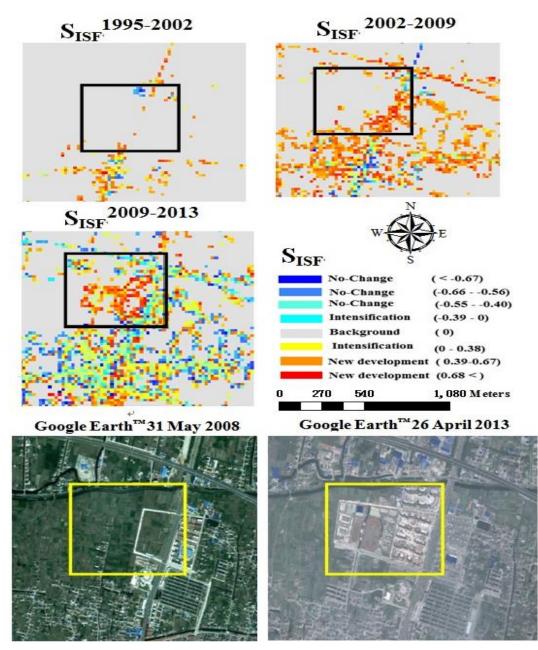
Fig.12.A portion of the CDZ illustrating the infilling of open spaces between existing impervious surfaces, the coordinate of this location is (30°16′50.79″N, 121°15′58.86″E)

5. Discussion

5.1 Methodological implications and limitations

There is both potential as well as limitations of the approach developed for impervious surface change analysis, particularly in the context of land use policy and ground transportation projects. Precisely quantifying the interaction between impervious surface change, transportation projects and land use policy is an important goal for remote sensing applications so as to help understand the causes of change and implement appropriate regulations. Up until recently, the impacts of different factors, such as land use policies and transportation on change in impervious surfaces were primarily explored through the use of thematic maps (Aljoufie et al., 2013a; Su et al., 2014; Ma et al., 2016; Song et al., 2016a; Zheng et al., 2016). These maps only provide a measure of conversion of non-urban land to urban cover types, i.e., urban growth (Dikou et al, Su et al, 2014). Despite the promising results, such maps might not appropriately represent change in impervious surfaces. Firstly, when urban landscapes are represented by a categorical land cover class this may lead to the loss of internal heterogeneity and cause a loss of information at the sub-pixel level which occurs particularly within urban cores (Herold et al., 2005; Myint and Lam, 2005; McGarigal et al., 2009). Secondly, thematic map techniques assign each pixel in a satellite sensor image to a single, most likely, class (Tatem et al., 2003). Change detection based on these results, can only quantify inter-class conversion (new urban areas) but not intra-class conversion (urban intensification), hence depicting an incomplete trajectory of urban dynamics (Yang and Liu, 2005). After all, urban attributes are inherently continuous in their spatial variation. Features such as impervious surfaces, soil, green spaces and other urban physical properties typically vary continuously over space and time. Hence, thematic maps might not reflect such properties in intelligent ways.

Compared to the thematic based change detection, quantifying impervious surface changes through the method proposed in this study provides useful information on the mechanisms of urban growth and urban intensification. Notably:(1) Statistical analysis measured the extent of new impervious surfaces, area of impervious surface fraction categories and changes in the overall magnitude of impervious surface fractions; (2) Characteristics of impervious surfaces were captured by means of MRA, which could attribute impervious surface changes to two major processes: urban growth and urban intensification. More specifically, the variability of approximation components defined urban growth whereas detail components represented intensification; (3) the TS slope(S_{ISF}) is an efficient tool for quantifying the spatial distribution of urban growth and intensification.

The additional information on the trajectory of change in impervious surface fraction may help to infer the processes involved in urban intensification. For instance, when the imperviousness declines over time, it is likely that high density urban areas such as old built-up areas have been transformed to modern high rise apartments during a redevelopment process (Fig.9). Simultaneous observation of both urban growth (e.g. expansion, infilling, and carpeting) and urban intensification (e.g., decline or increase of imperviousness) could be crucial for land use policy research. This is because such techniques provide a comprehensive representation of the interactions between urban development and land use regulations. In addition, if socio-economic variables or land use policy information are available at the grid level (e.g., pixels, or blocks), imperviousness can be statistically correlated to these variables. Thus this procedure has the potential to reveal unique insights into pattern–process relationships (Wu and Murray, 2005).

Although the results of this study are encouraging, care must be exercised when using this approach or similar techniques for mapping impervious surface change in the context of land use policy research. First, Landsat sensors (OLI, ETM+,and TM) have limited spatial resolution for quantifying impervious surfaces thereby these sensors might lead to anomalies, for example over-estimation of impervious surface area (Rashed, 2008). Second, assessing the accuracy of estimated impervious surface fraction does not incorporate a standard procedure compared to the thematic map approach. In general, the continuous results are evaluated using a range of metrics such as root mean square error and bias, which provide no specific information concerning user's accuracy and producer's accuracy of classes, which might be more difficult to comprehend for policy makers (Powell et al., 2007; Shahtahmassebi et al., 2014). However, change detection based on thematic maps includes standard accuracy assessment which generates a confusion matrix. In spite of these limitations, change detection based on the proposed method can comprehensively and intelligently depict the processes of urban growth and intensification.

5.2 Change detection analysis

The relationship between transportation and land use change has often been described as a "chicken-and-egg" problem since it is difficult to find out the trigger cause of change (Rodrigue et al., 2009). Therefore, we must stress that the Hangzhou Bay Bridge or any similar improved ground transportation systems may be only one of the many factors influencing the urban dynamics observed in this study. Thus any explanation that the bridge is directly responsible for urban growth and intensification is an over-simplification. However, the methodology and the results obtained from this study do much to facilitate a better understanding of the interaction between improved transportation projects, land use development policies, socio-economic variables and, thus, the growth of impervious surfaces.

5.2.1 Transportation projects as a catalyst for urban growth and intensification

Prior to constructing Hangzhou Bay Bridge, the Cixi County buffer zone included only a small amount of urban land (Fig. 5 and Fig.6). The accessibility of Cixi County to other regions of China was handicapped by mountains to the South and Hanghzou Bay to the North (Fig.2). With phases of development of the Hangzhou Bay Bridge, namely planning (1995-2002) and construction (2002-2009), the study area witnessed rapid expansion in urban area in the form of conversion of pervious lands to impervious surfaces. This form of growth was represented by positive S_{ISF} (Fig. 9) and approximation components of MRA (Fig.8-a) which can be observed mainly within rural areas and at the urban fringe(Fig. 7). Moreover, the total urban area increased markedly after the opening of Hangzhou Bay Bridge (2009-2013).

The rapid urban growth in Cixi County is consistent with national, provincial, municipal and local transportation policies (Fig.13). In terms of national policy, since 1995 the construction of a modernized comprehensive transport system has been accelerated in China in order to build a moderately prosperous society in all respects by 2020 (Chinese State Council, 2016) and such policies can stimulate urban growth. With respect to the provincial transportation regulations, many modern transportation projects such as super highway

networks, high speed train networks and a second mega sea bridge have been conducted in Zhejiang Province, particularly in the Hangzhou Bay region of this province. Given that Zhejiang province is one of the wealthiest and most powerful provinces in China, this province has given special attention to investment in such construction projects (Shira et al., 2012; Li, 2014). Consequently, this province and its Hangzhou Bay region witnessed faster growth in land used for transportation projects as a whole thereby such projects could speed up the urban growth (He et al., 2012). In addition, the Ningbo municipal government (Cixi County is a part of this municipality) has proposed a comprehensive transportation plan which promotes rapid expansion of transportation systems, particularly road networks, to support industrial regions and to encourage new urbanization (Ningbo_transportation_policy, 2015). It is noteworthy that since 2015 this plan has been implemented in this region and most of these road networks cross Cixi County and link to the Hangzhou Bay Bridge. Moreover, due to the Hangzhou Bay Bridge project, the local government of Cixi County has also implemented a range of improved transportation regulations such as increasing the length and quality of highways to connect Hangzhou Bay Bridge to other parts of China (Cixi_Traffic_Planning2002-2020, 2003). The accelerated construction of highways can also promote the expansion of built-up land along highway corridors and this has become a major driving force of urban growth. Highways across Cixi County have created a new spatial framework for regional development and this has promoted urban growth along the highways and existing urban fringe at the expense of mainly agricultural lands, as evidenced in Fig 11-yellow circle and ellipse.

National Level

Modernized comprehensive transport system | Promoting Economic and Social Development

Provincial Level,e.g., Zhejiang Province

Constructing modern transportation infrastructure | Example: Hangzhou Bay Bridge

Municipal level,e.g., Ningbo

Constructing ground transprotation infrastructure | Example:Exploiting advantages of the bridge

Local level,e.g., Cixi county

Constructing ground transprotation infrastructure | Example: Exploiting advantages of the bridge

Impacts

New developments(Figs 11 and 12): Converting pervious lands to impervious surfaces | Intensification(Fig. 10): Converting industrial regions to modern residential regions
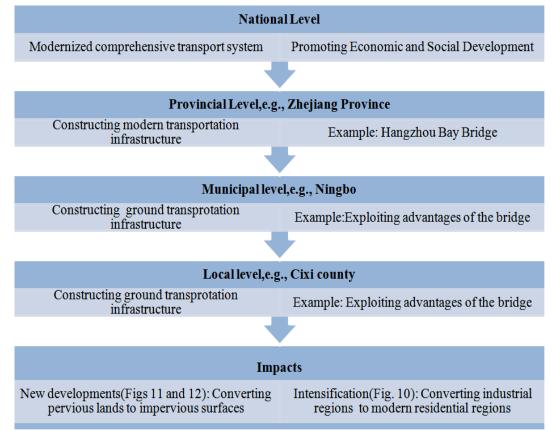
Fig.13. Cascade effects of national, provincial, municipal and local transportation policy on urban growth and intensification; see text for more detail. Also details of these policies can be found in: National level(Chinese

State Council, 2016),Provincial level(He et al., 2012),Municipal level(Ningbo_transportation_policy, 2015) and Local level (Cixi_Traffic_Planning2002-2020, 2003)

The second form of quantified change is urban intensification, as observed with moderate positive and negative values of S_{ISF}(Fig.9), reduction of detail components of MRA and, an increase and decrease in the magnitude of impervious surface fraction (Fig.8-b and Fig.8-c). The overall magnitude of impervious surface fraction increased between 1995-2009 (Fig.8-b, Fig.8-c and Fig.9), but we observed a decrease in the period 2009–2013 (Fig.8-b and Fig.8-c). Reduction or moderate change in imperviousness could suggest a redevelopment process which could be explained through observation, theory, renovation policies and local transportation regulations. First, our close visual inspection of Google Earth imagery showed that this phenomenon was generated by replacement of dense urban structures by more contemporary urban forms. As shown in Fig.10, old style urban structures such as factories generated large area and high impervious surface fractions whereas modern structures include hi-rise buildings but with new open spaces. Hence, urban intensification involving the conversion of old urban structures to the modern ones generated a reduction in impervious surface cover. The reduction of imperviousness in such areas is also congruent with urban neighborhood theory (Bourne, 1976; Rashed, 2008). Accordingly, urban development can be divided into five temporal stages: new growth, in-filling, stability, downgrading and thinning out, and renewal. Moderate change or decrease in imperviousness could be attributed to the thinning out stage in which cities are experiencing restructuring. In this stage, dense and old style urban landscapes decline and hi-rise buildings with wide open spaces increase. In terms of renovation policy, this phenomenon corresponds with the widespread motivation of policy makers in small towns on the eastern coast of China to encourage renovation or replacement of old and dense urban structures with new ones. The new developments are characterized by tall buildings, wide streets and green spaces within existing urban regions to attract investors to cities (Han, 2010). With respect to transportation policy, many factories in this region (Fig.10) have been moved to the urban fringes or along highways to exploit the advantages of new highways and corresponding links to the Hangzhou Bay Bridge as explained above (Fig.13).

5.2.2Transportation projects, socio-economic change and urban growth

Transportation infrastructure has a positive impact on the development of regions and economic growth (Lein and Day, 2008; Thomas and O'Donoghue, 2013). Also, transportation infrastructure brings trade and investment opportunities to previously unconnected regions (Mohmand et al., 2017). A range of studies have documented feedback relationships between the transportation system and local economic growth (Su et al., 2014; Song et al., 2016c). In particular, improved transportation systems attract new commercial and real estate projects that lead to a boom of economic development and population (e.g. Wang et al. (2017)).

In the present study, we found that GDP and highways have increased since the construction of the Hangzhou Bay Bridge (Table 6). The sharp increase of GDP suggests that the construction of the bridge promoted economic growth in the region. Growth of GDP in secondary and tertiary industries might reflect an increase in urban areas which accommodate industry and commercial services as well as the remarkable

economic development during the study period (Michishita et al., 2012). Zheng et al. (2016) demonstrated an increase in the number of foreign companies and industrial parks since the construction of the Hangzhou Bay Bridge which accords with the pattern of GDP growth observed in this study.

The results showed that the length of highway increased dramatically between 2002 and 2013. To connect Hangzhou Bay Bridge to other regions of China and maintain the pace of economic development, local government implemented powerful strategies to construct more highways in Cixi County. It is noteworthy that highway construction and associated development can lead to substantial increase in impervious surface land cover types (Ma et al., 2016). In fact, improved transportation projects such as Hangzhou Bay Bridge need to be connected to other regions, so these projects promote construction of other types of transportation systems such as highway and railways. Ultimately, they can cause rapid development of urban impervious surfaces.

Furthermore, during the study period the population increased slowly compared to urban growth. The differential growth rate between population and urban area is typical of urban sprawl which has been defined as a pattern of land-use/land-cover conversion in which the growth rate of urbanized land significantly exceeds the rate of population growth over a specific time period (Barnes et al., 2007; Powell et al., 2008b). Further, the construction of highways in the urban fringe for connecting Hangzhou Bay Bridge to other regions might have promoted sprawl. This finding was consistent with Zeng et al. (2015) who indicated that the construction of large transportation projects such as highways, railway stations, tunnels, and bridges in the fringes of the central districts have been linked to sprawl in China.

Table 6　Demographic and socio-economic conditions of Cixi County

a)　Economic conditions

Year	Gross GDP (billion RMB)	Growth of GDP (billion RMB)	GDP in secondary industry (billion RMB)	Growth of GDP in secondary industry (billion RMB)	GDP in tertiary industry (billion RMB)	Growth of GDP in tertiary industry (billion RMB)
1995	94.85	—	60.64	—	21.51	—
2002	211.97	117.12	123.58	62.94	71.22	49.71
2009	626.24	414.27	372.14	248.56	222.71	151.49
2013	1031.09	404.85	593.56	221.42	388.23	165.52

b)　Population and Highways

Year	Registered population (ten thousand)	Growth of population(ten thousand)	Highway length(km)	Growth of highway length (km)
1995	98.6	—	321.8	—
2002	100.5	1.9	478.8	157.0

| 2009 | 103.5 | 2.9 | 1299.8 | 821.0 |
| 2013 | 104.3 | 0.4 | 1554.3 | 254.5 |

5.2.3 Transportation projects, land use development policies and urban growth and intensification

With the Hangzhou Bay Bridge project, Cixi County could gradually become the transportation hub of eastern China, generating increasing population and economic growth. Therefore, one could argue that improved ground transportation projects are a driver of urban growth. However, this does not occur without the support of land use development policies. In fact, the growth of urban areas and ground transportation systems are part of a dynamic system that is subject to external influences. Consequently, the interactions between urban growth and transportation infrastructure are influenced by many factors such as land use policies, economics and demographics. In this context, policy factors play a crucial role as they can employ the development of ground transportation infrastructure as a growth catalyst which, in turn, results in urbanization (Erickson, 1995; Vickerman, 2015). We emphasize that the focus is on policy factors rather than planning, as policy factors have a much stronger relationship with legislation (Rodrigue et al., 2009). This holds true for China where policy has been an integral part of facilitating or inhibiting regional development. For instance, urban regions along the eastern coast of China were not developed between 1949 and 1978 partly because of security regulations at that time. However, after 1978 the architect of China's economic reform and open door policy Deng Xiao Ping promoted faster development of coastal regions as a way of spurring development in the interior regions (Yeung and Li, 2004).

In the context of the Hangzhou Bay Bridge project, both urban growth and urban intensification could be a consequence of provincial and local policies in this region to use the advantages of the bridge to promote local development by setting up the infrastructure ready for inside and outside investors. For example, promoting new urban developments can be reflected in provincial government guidelines which were announced after the opening of the bridge (Road_traffic, 2011):

"The bridge will help form a more convenient and efficient traffic network in the Yangtze River Delta, enabling each part to develop much closer relations with one another… We believe the bridge will open many more opportunities for the region's overall development and greatly enhance its economic strength and competitive power."

With respect to the urban intensification, since construction of Hangzhou Bay Bridge (2002) local government has implemented renovation policies to attract investors:

"Over the years we have committed ourselves to optimizing the investment environment and have fully promoted the new-type urbanization, in order to make Cixi County a more vigorous destination for investment."(Cixi_Government, 2013).

International experiences also highlight the interactions between policy factors and improved transportation which may promote or hinder regional development (Vickerman, 2015). For instance, development policies have encouraged new commercial and residential growth in Denmark and Sweden as a result of the Orsund Bridge. By contrast, the potential advantages of the Channel Tunnel for urban and commercial development in

the United Kingdom have been counterbalanced by domestic regulatory activities such as immigration control (Thomas and O'Donoghue, 2013).

In the introduction section, we proposed a conceptual model (Fig.1) which indicated an unknown relationship between improved transportation infrastructure and urban growth and intensification. Based on our findings, we now show a completed form of that model (Fig.14). The figure illustrates how improved transportation infrastructure interacts with development regulations, socio-economic variables and land use development policy. It should be noted that we postulate land use development policy may have a crucial role in this relationship as mentioned above (Vickerman, 2015). However, further efforts are needed to understand this relationship, and how those interconnections promote urban growth and intensification. Furthermore, care must be exercised about Fig. 14 as we supposed that improved transportation infrastructure based on the definition in the introduction is composed of high speed rail ways, super highways and mega sea bridg e(Zheng et al., 2016). Consequently, we did not focus on other types of improved ground transport projects such as installation of new metro systems or construction of heavy gauge rail lines. Further evaluation is warranted to explore the impacts of such projects on urban growth and intensification.
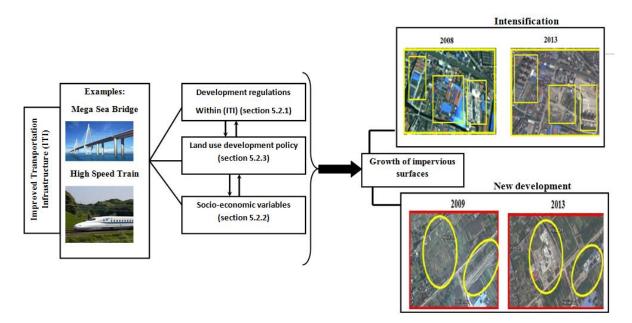

Fig.14. A conceptual model of the dynamic interactions between urban growth and intensification and improved transportation infrastructure.

5.3 Recommendations

One of the important concerns in land use policy research is for transportation infrastructure and its impacts on urbanization. As a result, authors such as Stone, (2004), Shahtahmassebi et al., (2014) and Ma et al., (2016) have highlighted the need for research to discover how driving forces such as transportation infrastructure, and land

use regulations lead to urban development (a policy investigation). Based on this and the findings of the present study, we identify the following requirements for future research:

1) From a technical perspective, more research is needed to develop continuous impervious surface change detection techniques that capture urban intensification (particularly redevelopment) and urban growth in the context of land use policy research.

2) From a conceptual point of view, future work should seek to establish direct casual mechanisms that link urban growth and intensification with land use policy, transportation projects and socio-economic variables. Such relationships would be a critical step towards devising a formal framework for understanding the driving forces of urban growth and intensification.

3) Many countries have focused on developing improved transportation infrastructure. Hence, there is an urgent need to adopt monitoring policies which take into account not only overall LULC change but specifically urban growth (incorporating infilling as well as expansion) and urban intensification (particularly redevelopment).

4) In this paper, we purposefully focused on the technical aspects of our work and analyzed the broad impacts of improved transportation projects such as Hangzhou Bay Bridge on urban growth and intensification. Future research should be targeted to explore in depth the local and regional effects of Hangzhou Bay Bridge on the surrounding regions particularly in terms of system thinking (Keesstra et al., 2018), planning support systems (Deal et al., 2017), scenario planning and sustainability (infrastructure and resource) (Deal and Pan, 2017).

6. Conclusions

There is a growing need to understand the interaction between transportation development projects and urban growth and intensification. In this respect, while several studies have focused on the impacts of improved transportation infrastructure on LULC change using thematic mapping techniques (Aljoufie et al., 2013a; Su et al., 2014; Song et al., 2016a), no studies have developed continuous frameworks for analyzing this relationship. Moreover, while efforts have been made to map urban changes (Weng, 2012; Shahtahmassebi et al., 2016; Song et al., 2016c), few studies have assessed the relationships between urban growth, urban intensification and land use policy. Thus, the present paper sought to address these issues directly.

Statistical techniques were employed to quantify areas of new impervious surfaces and changes in impervious surface fraction in urban and rural areas. We then used wavelet MRA to determine the overall patterns of urban development and intensification over time. Finally, the Theil-Sen slope technique was used to quantify the spatiotemporal dynamics of urban growth and intensification. Our results highlighted the value of mapping and monitoring urban changes using the proposed methods for understanding the dynamics of urban growth and intensification in the context of land use policies, specifically related to improved transportation infrastructure. A critical evaluation of the limitations and advantages of proposed methods for continuous change detection techniques was provided. Further research on the application of continuous change detection in land use policy research is warranted.

We assessed whether a new ground transportation project can encourage urban development and

intensification. To do this, the Hangzhou Bay Bridge was used as a representative of the type of large scale transportation development project that is increasingly found in China. One of the major goals of this bridge is to promote regional and local development. We observed substantial increases in urban area during (2002-2009) and after (2009-2013) the bridge construction in all major cities and rural regions within an analytical buffer zone in Cixi County. New urban developments mainly occurred on urban fringes and within rural regions at expense of agricultural lands. Although the overall magnitude of impervious surface fraction increased between 1995-2009, this value decreased in period 2009-2013 because of the transformation of old infrastructure in the urban cores via redevelopment as part of urban intensification schemes. In addition, we observed sharp increases in GDP, GDP in secondary industry, GDP in tertiary industry and length of highways during and after bridge construction. Both urban growth and intensification could be linked to improved transportation infrastructure projects. Overall, we found that transportation infrastructure developments can act upon land use development policies and socio-economic development like a chain reaction, as evidenced through the measurable urban growth and intensification over time. In this process, it is likely that land use development policies play an important role in either restricting or encouraging urban development through improved transportation projects. However, we must stress that more investigations are needed to detect the patterns associated with improved transportation infrastructure in China or elsewhere particularly based on conceptual frameworks such as systems thinking (Keesstra et al., 2018) and planning support systems (Deal et al., 2017).

The proposed analytical framework and outputs from a case study example offer a new perspective for relating urban development to transport, land use and economic policy. Such an approach is valuable for understanding the historical dynamics of growth and for monitoring and informing countries and regions that are currently undergoing rapid development.

Acknowledgements

References

Aksoy, E., Gultekin, N.T., 2006. Effects of transportation on urban development: Sivrihisar, Turkey. Wit Trans Built Env 89, 555-566.

Aljoufie, M., Zuidgeest, M., Brussel, M., van Maarseveen, M., 2013a. Spatial-temporal analysis of urban growth and transportation in Jeddah City, Saudi Arabia. Cities 31, 57-68.

Aljoufie, M., Zuidgeest, M., Brussel, M., van Vliet, J., van Maarseveen, M., 2013b. A cellular automata-based land use and transport interaction model applied to Jeddah, Saudi Arabia. Landscape Urban Plan 112, 89-99.

Badoe, D.A., Miller, E.J., 2000. Transportation-land-use interaction: empirical findings in North America, and their implications for modeling. Transport Res D-Tr E 5, 235-263.

Banerjee, A., Duflo, E., Qian, N., 2012. On the road: Access to transportation Infrastructure and Economic growth in China. The national bureau of economic research, NMER working Paper No. 1789 http://www.nber.org/papers/w17897(Accessed on 2.03.16)

Barnes, K.B., Morgan, J.M.I., Roberge, M.C., Lowe, S., 2007.
Sprawl development: its patterns, consequences, and measurement

Geospatial Research and Education Laboratory-Department of Geography and Environmental Planning https://www.researchgate.net/publication/251645410(Accessed on 25.6.17).

Bourne, L.S., 1976. Housing and supply and housing market behavior in residential development., in: Johnston, D.T.H.R.J. (Ed.), Social areas in cities – Vol 1: Spatial processes and form. Wiley, New York, pp. 111–158.

Bruschi, D., Garcia, D.A., Gugliermetti, F., Cumo, F., 2015. Characterizing the fragmentation level of Italian's National Parks due to transportation infrastructures. Transport Res D-Tr E 36, 18-28.

Cai, X.J., Wu, Z.F., Cheng, J., 2013. Using kernel density estimation to assess the spatial pattern of road density and its impact on landscape fragmentation. Int J Geogr Inf Sci 27, 222-230.

Castrence, M., Nong, D., Tran, C., Young, L., Fox, J., 2014. Mapping Urban Transitions Using Multi-Temporal Landsat and DMSP-OLS Night-Time Lights Imagery of the Red River Delta in Vietnam. Land 3, 148-166.

Chinese State Council, 2016. Chinese State Council. Chinese State Council website http://english.gov.cn/archive/white_paper/2016/12/29/content_281475528034734.htm Accessed on 25.06.17.

Chu, Q., Xu, Z.X., Peng, D.Z., Yang, X.J., Yang, G., 2015. Trends of surface humidity and temperature during 1951-2012 in Beijing, China. Iahs-Aish P 368, 126-131.

Cixi_Government, 2003. http://gh.cixi.gov.cn/art/2003/4/18/art_23390_355501.html, Accessed on 25.05.13.

Cixi_Government, 2013. http://www.cixi.gov.cn/art/2014/8/16/art_68144_1127797.html, Accessed on 25.05.15.

Cixi_Traffic_Planning2002-2020, 2003. http://gh.cixi.gov.cn/art/2003/4/18/art_23390_355501.html (Access on 12.7.17). In Chinese.

Deal, B., Pan, H.Z., 2017. Discerning and Addressing Environmental Failures in Policy Scenarios Using Planning Support System (PSS) Technologies. Sustainability-Basel 9.

Deal, B., Pan, H.Z., Pallathucheril, V., Fulton, G., 2017. Urban Resilience and Planning Support Systems: The Need for Sentience. J Urban Technol 24, 29-45.

Demarchi, L., Chan, J.C.W., Ma, J.L., Canters, F., 2012. Mapping impervious surfaces from superresolution enhanced CHRIS/Proba imagery using multiple endmember unmixing. Isprs J Photogramm 72, 99-112.

Dennison, P.E., Roberts, D.A., 2003. Endmember selection for multiple endmember spectral mixture analysis using endmember average RMSE. Remote Sens Environ 87, 123-135.

Erickson, D.L., 1995. Rural land use and land cover change. Land Use Policy 12, 223–236.

Freitas R.M, Y.E., S., 2008. Combining wavelets and linear spectral mixture model for MODIS satellite sensor time-series analysis. Journal of Computational Interdisciplinary Sciences 1, 51-56.

Galford, G.L., Mustard, J.F., Melillo, J., Gendrin, A., Cerri, C.C., Cerri, C.E.P., 2008. Wavelet analysis of MODIS time series to detect expansion and intensification of row-crop agriculture in Brazil. Remote Sens Environ 112, 576-587.

Gunasekera, K., Anderson, W., Lakshmanan, T.R., 2008. Highway-Induced Development: Evidence from Sri Lanka. World Dev 36, 2371-2389.

Han, S.S., 2010. Urban expansion in contemporary China: What can we learn from a small town? Land Use Policy 27, 780-787.

He, C., Huang, Z., Wang, W., 2012. Land use changes and economic growth in China. Lincoln Institute of Land Policy,Land Lines.

Herold, M., Couclelis, H., Clarke, K.C., 2005. The role of spatial metrics in the analysis and modeling of urban land use change. Computers, Environment and Urban Systems 29, 369-399.

Hubbard, B.B., 1998. The world according to wavelets : the story of a mathematical technique in the making, 2nd ed. A.K. Peters, Wellesley, Mass.

IDRISI, H.o., 2012. IDRISI Selva 17.

Jha, M.K., Ogallo, H.G., Owolabi, O., 2014. A Quantitative Analysis of Sustainability and Green Transportation Initiatives in Highway Design and Maintenance. Procd Soc Behv 111, 1185-1194.

Jia, R., Guo, X., Marinova, D., 2012. The role of the clean development mechanism in achieving China's goal of a resource-efficient and environmentally friendly society. Environment, Development and Sustainability 15, 133-148.

Jiang, W.G., Yuan, L.H., Wang, W.J., Cao, R., Zhang, Y.F., Shen, W.M., 2015. Spatio-temporal analysis of vegetation variation in the Yellow River Basin. Ecol Indic 51, 117-126.

Keesstra, S., Nunes, J., Novara, A., Finger, D., Avelar, D., Kalantari, Z., Cerda, A., 2018. The superior effect of nature based solutions in land management for enhancing ecosystem services. Sci Total Environ 610, 997-1009.

Kim, J.Y., Han, J.H., 2016. Straw effects of new highway construction on local population and employment growth. Habitat Int 53, 123-132.

Lein, J.K., Day, K.L., 2008. Assessing the growth-inducing impact of the Appalachian Development Highway System in southern Ohio: Did policy promote change? Land Use Policy 25, 523-532.

Li, H.R., 2016. Study on Green Transportation System of International Metropolises. Procedia Engineer 138, 762-771.

Li, L., 2014. Logistics Development in Zhejiang Province, in: Liu B., Lee S., Wang L., Xu Y., X., L. (Eds.), Contemporary Logistics in China. Current Chinese Economic Report Series. Springer, Berlin, Heidelberg, pp. 65-83.

Lichtenberg, E., Ding, C.G., 2008. Assessing farmland protection policy in China. Land Use Policy 25, 59-68.

Lindsay, R.W., Percival, D.B., Rothrock, D.A., 1996. The discrete wavelet transform and the scale analysis of the surface properties of sea ice. Ieee T Geosci Remote 34, 771-787.

Locatelli, G., Invernizzi, D.C., Brookes, N.J., 2017. Project characteristics and performance in Europe: An empirical analysis for large transport infrastructure projects. Transport Res a-Pol 98, 108-122.

Loo, B.P.Y., 1999. Development of a regional transport infrastructure: some lessons from the Zhujiang Delta, Guangdong, China. J. Transp. Geogr 7, 43-63.

Lu, D.S., Weng, Q.H., 2006. Use of impervious surface in urban land-use classification. Remote Sens Environ 102, 146-160.

Ma, Q., He, C.Y., Wu, J.G., 2016. Behind the rapid expansion of urban impervious surfaces in China: Major influencing factors revealed by a hierarchical multiscale analysis. Land Use Policy 59, 434-445.

Martinez, B., Gilabert, M.A., 2009. Vegetation dynamics from NDVI time series analysis using the wavelet transform. Remote Sens Environ 113, 1823-1842.

Martinez, B., Gilabert, M.A., Garcia-Haro, F.J., Faye, A., Melia, J., 2011. Characterizing land condition variability in Ferlo, Senegal (2001-2009) using multi-temporal 1-km Apparent Green Cover (AGC) SPOT Vegetation data. Global Planet Change 76, 152-165.

McGarigal, K., Tagil, S., Cushman, S.A., 2009. Surface metrics: an alternative to patch metrics for the quantification of landscape structure. Landscape Ecol 24, 433-450.

Michishita, R., Jiang, Z.B., Xu, B., 2012. Monitoring two decades of urbanization in the Poyang Lake area, China through spectral unmixing. Remote Sens Environ 117, 3-18.

Mohmand, Y.T., Wang, A.H., Saeed, A., 2017. The impact of transportation infrastructure on economic growth: empirical evidence from Pakistan. Transp Lett 9, 63-69.

Myint, S.W., Lam, N., 2005. A study of lacunarity-based texture analysis approaches to improve urban image classification. Computers, Environment and Urban Systems 29, 501-523.

Percival, D.B., Walden, A.T., 2000. Wavelet methods for time series analysis. Cambridge University Press, Cambridge ; New York.

Powell, R., Roberts, D., 2010. Characterizing urban land-cover change in Brazil. J.Latin Am. Geogr. 9, 183–211.

Powell, R.L., Roberts, D.A., 2008a. Characterizing Variability of the Urban Physical Environment for a Suite of Cities in Rondonia, Brazil. Earth Interact 12.

Powell, R.L., Roberts, D.A., Dennison, P.E., Hess, L.L., 2007. Sub-pixel mapping of urban land cover using multiple endmember spectral mixture analysis: Manaus, Brazil. Remote Sens Environ 106, 253-267.

Powell, S.L., Cohen, W.B., Yang, Z., Pierce, J.D., Alberti, M., 2008b. Quantification of impervious surface in the Snohomish Water Resources Inventory Area of Western Washington from 1972-2006. Remote Sens Environ 112, 1895-1908.

Rashed, T., 2008. Remote sensing of within-class change in urban neighborhood structures. Comput Environ Urban 32, 343-354.

Road_traffic, 2011. http://www.roadtraffic-technology.com/projects/hangzhou/(Accessed on 25.05.15).

Roberts, D., Halligan, K., & Dennison, P. (2007). , 2007. VIPER tools user manual. Version 1.2. www.vipertools.org(Accessed on 04.04.11).

Rodrigue, J.-P., Comtois, C., Slack, B., 2009. The geography of transport systems, 2nd ed. Routledge, London ; New York.

Serrano, M., Sanz, L., Puig, J., Pons, J., 2002. Landscape fragmentation caused by the transport network in Navarra (Spain) - Two-scale analysis and landscape integration assessment. Landscape Urban Plan 58, 113-123.

Shahtahmassebi, A., Pan, Y., Lin, L., Shortridge, A., Wang, K., Wu, J.X., Wu, D., Zhang, J., 2014. Implications of land use policy on impervious surface cover change in Cixi County, Zhejiang Province, China. Cities 39, 21-36.

Shahtahmassebi, A., Yu, Z.L., Wang, K., Xu, H.W., Deng, J.S., Li, J.D., Luo, R.S., Wu, J., Moore, N., 2012. Monitoring rapid urban expansion using a multi-temporal RGB-impervious surface model. J Zhejiang Univ-Sc A 13, 146-158.

Shahtahmassebi, A.R., Song, J., Zheng, Q., Blackburn, G.A., Wang, K., Huang, L.Y., Pan, Y., Moore, N., Shahtahmassebi, G., Sadrabadi Haghighi, R., Deng, J.S., 2016. Remote sensing of impervious surface growth: A framework for quantifying urban expansion and re-densification mechanisms. International Journal of Applied Earth Observation and Geoinformation 46, 94-112.

Shira, D., Devonshire-Ellis C., Jones S, E., K., 2012. Provinces and Cities of the YRD, in: Shira, D., , D.-E.C., , J.S., Ku E. (Eds.), The Yangtze River Delta. China Briefing (The Practical Application of China Business). Springer, Berlin,

Heidelberg, pp. 64-86.

Song, J., Ye, J., Zhu, E., Deng, J., Wang, K., 2016a. Analyzing the Impact of Highways Associated with Farmland Loss under Rapid Urbanization. ISPRS International Journal of Geo-Information 5, 94.

Song, M.L., Zhang, G.J., Zeng, W.X., Liu, J.H., Fang, K.N., 2016b. Railway transportation and environmental efficiency in China. Transport Res D-Tr E 48, 488-498.

Song, X.-P., Sexton, J.O., Huang, C., Channan, S., Townshend, J.R., 2016c. Characterizing the magnitude, timing and duration of urban growth from time series of Landsat-based estimates of impervious cover. Remote Sens Environ 175, 1-13.

Stone, B., 2004. Paving over paradise: how land use regulations promote residential imperviousness. Landscape Urban Plan 69, 101-113.

Su, S.L., Xiao, R., Li, D.L., Hu, Y.N., 2014. Impacts of Transportation Routes on Landscape Diversity: A Comparison of Different Route Types and Their Combined Effects. Environ Manage 53, 636-647.

Sung, C.Y., Yi, Y.J., Li, M.H., 2013. Impervious surface regulation and urban sprawl as its unintended consequence. Land Use Policy 32, 317-323.

Tatem, A.J., Lewis, H.G., Atkinson, P.M., Nixon, M.S., 2003. Increasing the spatial resolution of agricultural land cover maps using a Hopfield neural network. Int J Geogr Inf Sci 17, 647-672.

Thomas, P., O'Donoghue, D., 2013. The Channel Tunnel: transport patterns and regional impacts. J Transp Geogr 31, 104-112.

Thorp, K.R., French, A.N., Rango, A., 2013. Effect of image spatial and spectral characteristics on mapping semi-arid rangeland vegetation using multiple endmember spectral mixture analysis (MESMA). Remote Sens Environ 132, 120-130.

Tsou, K.W., Cheng, H.T., Tseng, F.Y., 2015. Exploring the relationship between multilevel highway networks and local development patterns-a case study of Taiwan. J Transp Geogr 43, 160-170.

Vickerman, R., 2015. High-speed rail and regional development: the case of intermediate stations. J Transp Geogr 42, 157-165.

Wang, Z.B., Xu, G., Bao, C., Xu, J.B., Sun, F.H., 2017. Spatial and economic effects of the Bohai Strait Cross-Sea Channel on the transportation accessibility in China. Appl Geogr 83, 86-99.

Weng, Q., 2008. Remote sensing of impervious surfaces. CRC Press, Boca Raton.

Weng, Q.H., 2012. Remote sensing of impervious surfaces in the urban areas: Requirements, methods, and trends. Remote Sens Environ 117, 34-49.

Wilkins, K., Zurawski, K., 2014. Infrastructure Investment in China Bulletin, Reserve Bank of Australia. Retrieved July 2015.

Wu, C., Murray, A.T., 2005. A cokriging method for estimating population density in urban areas. Computers, Environment and Urban Systems 29, 558-579.

Yang, L.M., Xian, G., Klaver, J.M., Deal, B., 2003. Urban land-cover change detection through sub-pixel imperviousness mapping using remotely sensed data. Photogramm Eng Rem S 69, 1003-1010.

Yang, X., Liu, Z., 2005. Use of satellite-derived landscape imperviousness index to characterize urban spatial growth. Computers, Environment and Urban Systems 29, 524-540.

Yeung, Y.M., Li, X.J., 2004. China's western development: The role of the state in historical and regional perspective. Shanghai-Hong Kong Development Institute 10.

Zeng, C., Liu, Y.L., Stein, A., Jiao, L.M., 2015. Characterization and spatial modeling of urban sprawl in the Wuhan Metropolitan Area, China. International Journal of Applied Earth Observation and Geoinformation 34, 10-24.

Zheng, Q., He, S., Huang, L.Y., Zheng, X.Y., Pan, Y., Shahtahmassebi, A.R., Shen, Z.Q., Yu, Z.L., Wang, K., 2016.

Assessing the Impacts of Chinese Sustainable Ground Transportation on the Dynamics of Urban Growth: A Case Study of the Hangzhou Bay Bridge. Sustainability-Basel 8.